

## Enhancement of critical current density in Co-doped BaFe<sub>2</sub>As<sub>2</sub> with columnar defects introduced by heavy-ion irradiation

Y. Nakajima,<sup>1,2</sup> Y. Tsuchiya,<sup>1</sup> T. Taen,<sup>1</sup> T. Tamegai,<sup>1,2</sup> S. Okayasu,<sup>3</sup> and M. Sasase<sup>4</sup>

<sup>1</sup>*Department of Applied Physics, The University of Tokyo, Hongo, Bunkyo-ku, Tokyo 113-8656, Japan*

<sup>2</sup>*JST, Transformative Research-Project on Iron Pnictides (TRIP), 7-3-1 Hongo, Bunkyo-ku, Tokyo 113-8656, Japan*

<sup>3</sup>*Advanced Science Research Center, Japan Atomic Energy Agency, Tokai, Ibaraki 319-1195, Japan*

<sup>4</sup>*The Wakasa-wan Energy Research Center, Research and Development Group, 64-52-1 Nagatani, Tsuruga, Fukui 914-0192, Japan*  
(Received 26 June 2009; published 30 July 2009)

We report the realization of columnar defects in Co-doped BaFe<sub>2</sub>As<sub>2</sub> single crystal by heavy-ion irradiation. The columnar defects are confirmed by transmission electron microscopy, and their density is about 40% of the irradiation dose. Magneto-optical imaging and bulk magnetization measurements reveal that the critical current density is strongly enhanced in the irradiated region. We also find that vortex creep rates are strongly suppressed by the columnar defects. We compare the effect of heavy-ion irradiation into Co-doped BaFe<sub>2</sub>As<sub>2</sub> and cuprate superconductors.

DOI: [10.1103/PhysRevB.80.012510](https://doi.org/10.1103/PhysRevB.80.012510)

PACS number(s): 74.25.Qt, 74.25.Sv, 74.70.Dd

A limitation on the technological advances of high-temperature superconductors comes from the intrinsically low critical current density  $J_c$ . Recently discovered iron-based superconductors<sup>1</sup> also face the same problem. While the transition temperature  $T_c$  is increased up to  $\sim 55$  K in rare-earth-based iron-oxyarsenides within a short period of time,<sup>2</sup>  $J_c$  at low temperatures is still low.<sup>3-5</sup> Although the transition temperature of iron-pnictide superconductors is still lower than cuprate superconductors, the introduction of pinning centers can enhance the critical current density and make this system more attractive for practical applications. It is well known that the most efficient way to improve the critical current density is to pin the vortices with columnar defects created by swift particle irradiation. In high-temperature superconductors, columnar defects enhance  $J_c$  dramatically.<sup>6,7</sup>

Intermetallic iron-arsenide Ba(Fe<sub>1-x</sub>Co<sub>x</sub>)<sub>2</sub>As<sub>2</sub> with  $T_c \sim 24$  K is readily available in large single crystalline form,<sup>8</sup> and its  $J_c$  reaches  $10^6$  A/cm<sup>2</sup> at  $T=2$  K, which is potentially attractive for technological applications.<sup>3-5</sup> We expect that  $J_c$  in Ba(Fe<sub>1-x</sub>Co<sub>x</sub>)<sub>2</sub>As<sub>2</sub> could be enhanced by introducing columnar defects that can pin the vortices. However, it is well known that irradiation-induced defects strongly depend on various parameters such as ion energy, stopping power of incident ions, thermal conductivity, and perfection of the target crystal, etc.<sup>9</sup> Since there are so many influencing factors, it is still an open question whether irradiation damage can be introduced in iron-arsenide superconductors. In this Brief Report, we report an attempt to create the columnar defects by heavy-ion irradiation into Co-doped BaFe<sub>2</sub>As<sub>2</sub> single crystals. Columnar tracks with diameters of  $\sim 2-5$  nm and about 40% of nominal ion dose are clearly seen in scanning transmission electron microscopy (STEM) images. Magneto-optical images and bulk magnetization measurements reveal a strong enhancement of  $J_c$  in the irradiated region. Columnar defects also suppress the relaxation of magnetization consistent with the enhancement of pinning capability of vortices. Effect of columnar defects on the vortex dynamics is compared between Co-doped BaFe<sub>2</sub>As<sub>2</sub> and high-temperature superconductors.

Single crystalline samples of Ba(Fe<sub>0.93</sub>Co<sub>0.07</sub>)<sub>2</sub>As<sub>2</sub> were

grown by FeAs/CoAs self-flux method.<sup>5</sup> Co concentration was determined by energy dispersive x-ray (EDX) spectroscopy measurements. 200 MeV Au ions were irradiated into Ba(Fe<sub>0.93</sub>Co<sub>0.07</sub>)<sub>2</sub>As<sub>2</sub> along  $c$  axis using the tandem accelerator in JAEA to create columnar defects. In order to maximize the effect of irradiation, crystals with thicknesses  $\sim 10$   $\mu$ m were irradiated considering the penetration depth of 200 MeV Au ions into Ba(Fe<sub>0.93</sub>Co<sub>0.07</sub>)<sub>2</sub>As<sub>2</sub>, 8.5  $\mu$ m. Field-equivalent defect densities, matching field, is  $B_\phi=20$  kG. Plan view and cross-sectional observations of the irradiated Ba(Fe<sub>0.93</sub>Co<sub>0.07</sub>)<sub>2</sub>As<sub>2</sub> were performed with a high-resolution and scanning TEM (JEOL, JEM-3000F). Magnetization was measured by a commercial superconducting quantum interference device (SQUID) magnetometer (MPMS-XL5, Quantum Design). Magneto-optical images were obtained by using the local-field-dependent Faraday effect in the in-plane magnetized garnet indicator film employing a differential method.<sup>10,11</sup>

Figure 1(a) shows a plan view of the irradiated Ba(Fe<sub>0.93</sub>Co<sub>0.07</sub>)<sub>2</sub>As<sub>2</sub> along  $c$  axis, where defects are marked by dotted circles. The density of defects extracted from the average of ten different regions is  $4.2 \pm 1.2 \times 10^{10}$  cm<sup>-2</sup>, which is about 40% of the expected value. High-resolution TEM observation shown in the inset of Fig. 1(a) reveals that the size of defects is  $\sim 2-5$  nm with a large fluctuation, and the lattice image is sustained with some displacements of atoms. Such characteristics of heavy-ion-induced defects makes a good contrast to amorphous defects with diameters  $\sim 10$  nm created in high-temperature cuprate superconductors.<sup>9</sup> The morphology of defects along the projectile is clearly columnar as identified in the cross sectional image shown in Fig. 1(b). However, columnar defects are discontinuous with various lengths ranging 30–240 nm. We also note that our preliminary measurements on Ba(Fe<sub>0.93</sub>Co<sub>0.07</sub>)<sub>2</sub>As<sub>2</sub> irradiated by 200 MeV Ni ions give reduced effect on its electromagnetic properties. All these experimental facts suggests that 200 MeV Au irradiation is marginal to create continuous columnar defects in Ba(Fe<sub>0.93</sub>Co<sub>0.07</sub>)<sub>2</sub>As<sub>2</sub>. Creation of columnar defects are controlled by various factors, such as mass and energy of heavy ions, thermal conductivity, and carrier density of the system.

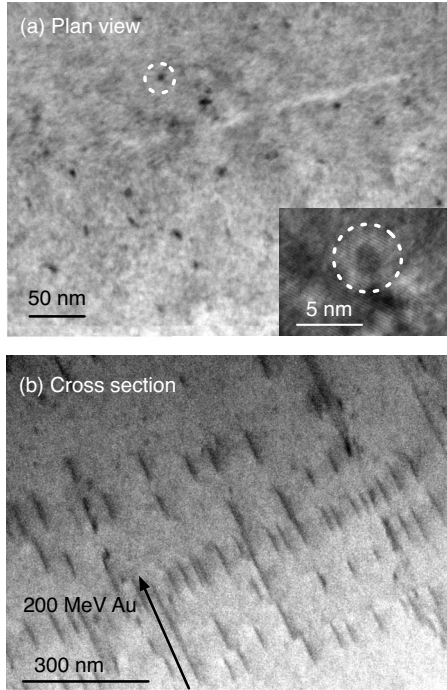


FIG. 1. STEM observation of an irradiated  $\text{Ba}(\text{Fe}_{0.93}\text{Co}_{0.07})_2\text{As}_2$ . (a) Plan view. Dotted circle indicates the columnar defect with average density of  $4.2 \pm 1.2 \times 10^{10} \text{ cm}^{-2}$ , which corresponds to about 40% of the expected value. Inset: high-resolution TEM image (different region). (b) Cross section. The arrow indicates the direction of 200 MeV Au irradiation, which corresponds to  $c$  axis.

It would be of great interest to compare the defect characteristics created by lighter and heavier ions.

Enhancements of vortex pinning introduced by the irradiation are directly visualized by magneto-optical imaging. The inset of Fig. 2(a) shows an optical image of  $\text{Ba}(\text{Fe}_{0.93}\text{Co}_{0.07})_2\text{As}_2$ . For comparison, we covered a half of the crystal by Au foil with a thickness of  $100 \mu\text{m}$  and the rest half is irradiated. The left area inside the rectangle is irradiated region. We note that  $T_c$  of the irradiated  $\text{Ba}(\text{Fe}_{0.93}\text{Co}_{0.07})_2\text{As}_2$  sample is 24 K and is not affected by the introduction of the columnar damage. The main panel of Fig. 2(a) shows a magneto-optical image in the remanent state of  $\text{Ba}(\text{Fe}_{0.93}\text{Co}_{0.07})_2\text{As}_2$  at 5 K after increasing field up to 800 Oe for 5 s and reducing it to zero. We find prominent difference of vortex penetrations between the irradiated and unirradiated regions. In the unirradiated region, vortices penetrate deep into the sample in addition to the penetration from a defect on the top edge. By contrast, the penetration in the irradiated region is much reduced than those in the unirradiated region, which indicates that defects introduced by the irradiation enhance the vortex pinning in the irradiated region. In fact, critical current density in the irradiated region is strongly enhanced. Line profile obtained from Fig. 2(a) is plotted in Fig. 2(b). The critical current density can be roughly estimated using the equation,

$$J_c = \frac{c}{4d} \frac{H_{ex}}{\cosh^{-1}[w/(w-2p)]}, \quad (1)$$

where  $H_{ex}$  is external field,  $w$  is the sample width,  $d$  is the sample thickness, and  $p$  is the penetration with measured

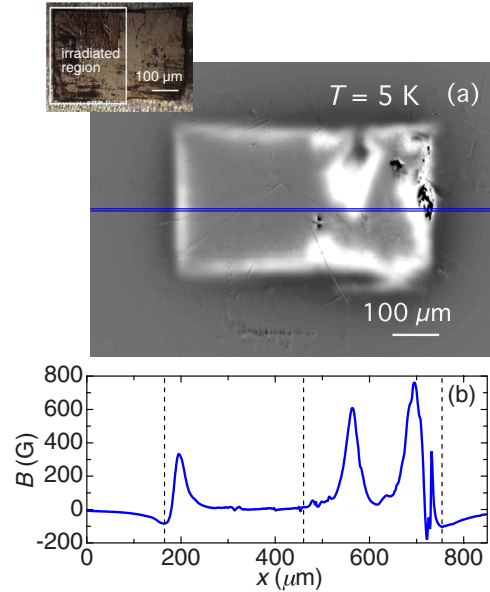


FIG. 2. (Color online) (a) Magneto-optical image of the remanent state in  $\text{Ba}(\text{Fe}_{0.93}\text{Co}_{0.07})_2\text{As}_2$  at 5 K. The inset shows the optical image of  $\text{Ba}(\text{Fe}_{0.93}\text{Co}_{0.07})_2\text{As}_2$ . The area surrounded by the rectangle is the region irradiated by 200 MeV Au ions. (b) Line profile along a line in (a). Broken lines show locations of sample edges and the irradiation boundary.

from the sample edge.<sup>12</sup> From this equation with the width of the irradiated region  $w=295 \mu\text{m}$ ,  $d=10 \mu\text{m}$ , and  $p=59 \mu\text{m}$ , we can roughly estimate  $J_c$  as  $\sim 1.8 \times 10^6 \text{ A/cm}^2$  in the irradiated region, which is much larger than that in the unirradiated sample<sup>3-5</sup> and demonstrates the effectiveness of columnar defects for vortex pinning in Co-doped  $\text{BaFe}_2\text{As}_2$ .

We can also confirm the enhancement of flux pinning by the bulk magnetization measurements. To evaluate the magnetization precisely, we separated the irradiated region by carefully cutting the half-irradiated sample. Insets of Figs. 3(a) and 3(b) show the magnetization curves at several temperatures in the unirradiated and irradiated samples, respectively. In the unirradiated sample, pronounced fish-tail effect is observed at higher temperatures and the peak at zero field is very sharp.<sup>3-5</sup> By contrast, the magnetization in the irradiated sample is enhanced in spite of much smaller size and the fish-tail effect is absent. The peak at zero field is broadened due to the drastic increase in low-field irreversible magnetization. We note that in high- $T_c$  cuprates a peak near  $\sim B_\phi/3$  in magnetization is observed.<sup>13,14</sup> In this system, however, the prominent peak of irreversible magnetization at  $\sim B_\phi/3$  may be absent or very small.

The bulk critical current density  $J_c$  is derived from the Bean model,

$$J_c = 20 \frac{\Delta M}{a(1-b/3a)}, \quad (2)$$

where  $\Delta M$  is  $M_{down} - M_{up}$ ,  $M_{up}$  and  $M_{down}$  are the magnetization when sweeping fields up and down, respectively, and  $a$  and  $b$  are the sample widths ( $a < b$ ). Figures 3(a) and 3(b) show the field dependence of  $J_c$  in the unirradiated and irradiated samples, respectively. In the unirradiated sample,  $J_c$  is

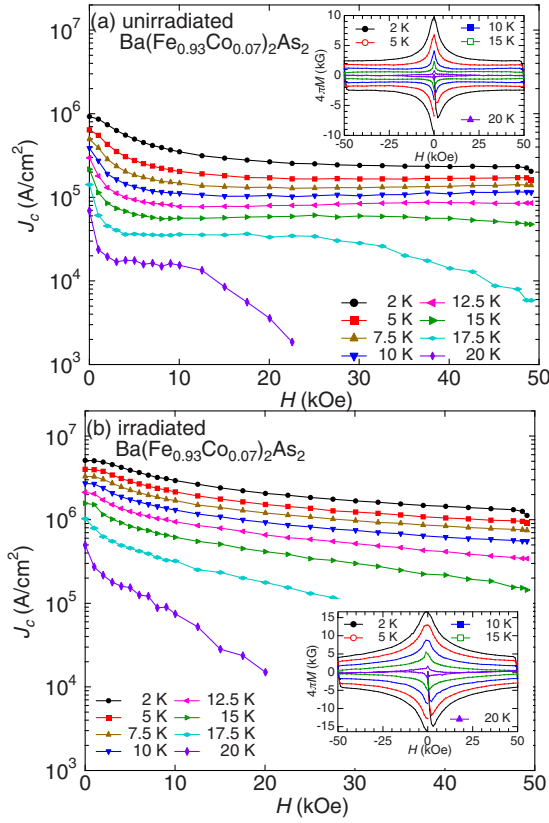


FIG. 3. (Color online) Field dependence of critical current density calculated by Eq. (2) at several temperatures in (a) the unirradiated ( $450 \times 584 \times 30 \mu\text{m}^3$ ) and (b) the irradiated ( $164 \times 309 \times 10 \mu\text{m}^3$ )  $\text{Ba}(\text{Fe}_{0.93}\text{Co}_{0.07})_2\text{As}_2$ . Inset: field dependence of the magnetization at several temperatures in the unirradiated and irradiated  $\text{Ba}(\text{Fe}_{0.93}\text{Co}_{0.07})_2\text{As}_2$ .

about  $6.4 \times 10^5 \text{ A/cm}^2$  at  $T=5 \text{ K}$  under zero applied field. At high temperatures  $J_c$  changes nonmonotonically with magnetic field reflecting the fish-tail effect in magnetization. In the irradiated sample, a drastic enhancement of  $J_c$  is observed in the whole temperature and field range.  $J_c$  in the irradiated sample at  $T=5 \text{ K}$  under zero field reaches  $4.0 \times 10^6 \text{ A/cm}^2$ .  $J_c$  in the irradiated sample decreases monotonically with increasing magnetic field. These results obtained from bulk magnetization measurements also indicate that heavy-ion irradiation introduces pinning centers for vortices.

To get insight into vortex dynamics, we investigate the relaxation of shielding current. Figure 4 shows the normalized relaxation rate  $S$  defined by  $S = |d \ln M / d \ln t|$  in the remanent state of the unirradiated and irradiated samples. In the unirradiated sample,  $S$  shows a broad peak around  $T \sim 8 \text{ K}$ . This behavior is qualitatively similar to that reported in Ref. 3. By contrast,  $S$  in the irradiated sample is strongly suppressed at all temperatures, which demonstrates the effect of columnar defects on flux creep. With increasing temperature,  $S$  in the irradiated sample increases monotonically and approaches to that in the unirradiated sample at temperatures close to  $T_c$ , which indicate that additional flux pinning by columnar defects is reduced by thermal fluctuations. It should be noted that  $S$  shows a steep increase close to zero field in the unirradiated sample. The peak of  $S$  around 8 K in

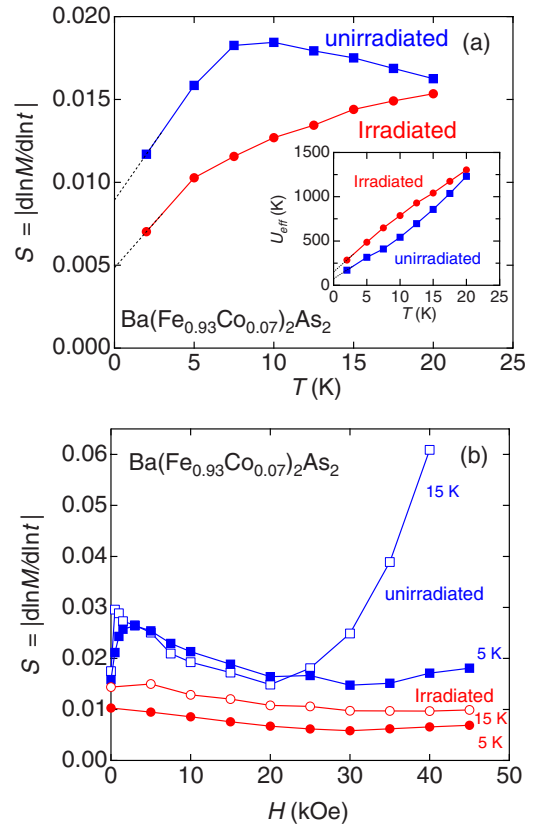


FIG. 4. (Color online) (a) Temperature dependence of normalized relaxation rate  $S = |d \ln M / d \ln t|$  in the unirradiated and irradiated  $\text{Ba}(\text{Fe}_{0.93}\text{Co}_{0.07})_2\text{As}_2$  in the remanent state. Dotted lines are linear extrapolations down to  $T=0 \text{ K}$ . Inset: temperature dependence of effective pinning energy  $U_{\text{eff}} = T/S$  in the unirradiated and the irradiated  $\text{Ba}(\text{Fe}_{0.93}\text{Co}_{0.07})_2\text{As}_2$ . Dotted lines are linear extrapolations down to  $T=0 \text{ K}$ . (b) Field dependence of  $S$  in the unirradiated and irradiated  $\text{Ba}(\text{Fe}_{0.93}\text{Co}_{0.07})_2\text{As}_2$  at 5 and 15 K.

the unirradiated sample could be related to this low-field anomaly. Namely, as temperature is lowered, trapped field in the sample increases, inducing the increase in  $S$  in average due to the intrinsic field dependence of  $S$ . In fact, the temperature dependence of  $S$  in the irradiated sample, where no low-field increase is observed, does not show a maximum. We note that in  $\text{YBa}_2\text{Cu}_3\text{O}_{7-\delta}$ , temperature-independent plateau in the normalized relaxation rate with values in the range  $S=0.020-0.035$ , similar to the present value, is observed and interpreted in terms of collective creep theory.<sup>15</sup>

To get further insight, we estimate the pinning energy  $U_{\text{eff}}$  using the conventional flux creep relation

$$M = M_0 \left( 1 - \frac{T}{U_{\text{eff}}} \ln(t/t_0) \right), \quad (3)$$

where  $t_0$  is the vortex-hopping attempt time. From this relation, effective pinning energy is obtained as  $U_{\text{eff}} = T/S$ . The inset of Fig. 4(a) shows the temperature dependence of  $U_{\text{eff}}$  in the unirradiated and irradiated samples.  $U_{\text{eff}}$  in both samples increases almost linearly with temperature, which is similar to that in oxypnictide superconductor  $\text{SmFeAsO}_{0.9}\text{F}_{0.1}$ .<sup>16</sup> Enhancement of  $U_{\text{eff}}$  by the columnar de-

